

Microscopic Nonaffine Deformation of Polydisperse Polymer Networks

G. Glatting,* R. G. Winkler,[†] and P. Reineker[‡]

Abteilung Nuklearmedizin, Universität Ulm, Robert-Koch-Strasse 8, 89081 Ulm, Germany

Received November 28, 1994; Revised Manuscript Received April 18, 1995*

ABSTRACT: The stress–strain behavior of polydisperse networks is investigated using the maximum entropy principle. The network is described as a gas of phantom chains, and the deformation is taken into account by macroscopic constraints. Thus, nonaffine deformation on a microscopic scale is allowed and occurs. The main experimental features are reproduced, without introducing parameters additional to the strand number. In addition, the length distribution of network strands in a polymerization reaction is calculated. An exponential distribution of chain lengths is found.

1. Introduction

Polymer networks are widely used for technological applications; their large reversible elasticity is one of the reasons. Most theoretical models^{1–9} assume for these networks identical network strands, i.e., these models describe monodisperse or unimodal networks. However, the technically applied networks mostly possess a broad distribution of strand lengths; i.e., they are polydisperse or bi- and multimodal. Recently,^{7–9} we introduced a new description of monodisperse or unimodal polymer networks. In this paper we extend this model to polydisperse networks. Network vacancies, as for example, dangling bonds, loops, or double connection of cross-links (see e.g. ref 7), are not included in our model, because they do not contribute to the elastic energy.

In the next section we introduce the model for a bimodal polymer network consisting of Gaussian chains of different lengths. We compare the biaxial stress–strain relation with experimental data and investigate the behavior of both chain ensembles under strain. In the third section a polydisperse network is investigated, which assumes an extremum of entropy under the constraints of given monomer and strand numbers. We calculate the distribution of strand lengths and the stress–strain behavior. Section 4 gives the conclusion.

2. Bimodal Network

Two ensembles ($j = 1, 2$) of equivalent and noninteracting strands, differing only in their contour length, with strand entropies $k_B S_{sj}(\bar{r})$, distributed between the allowed cross-links of the given network, yield the entropy of the total network (compare refs 7–9)

$$S_{\text{net}}(\Lambda) = k_B \sum_{j=1}^2 \int M_j(\bar{r}) S_{sj}(\bar{r}) d^3r + k_B \sum_{j=1}^2 \{M_j \ln M_j - \int M_j(\bar{r}) \ln M_j(\bar{r}) d^3r\} + k_B \sum_{j=1}^2 (\mu_j - 1) \{M_j - \int M_j(\bar{r}) d^3r\} + k_B \sum_{i=1}^n \gamma_i \sum_{j=1}^2 \left\{ \int M_j(\bar{r}) g_i(\bar{r}) d^3r - \int M_{0j}(\bar{r}) g_i(\Lambda \bar{r}) d^3r \right\} \quad (1)$$

$M_j(\bar{r})$ is the number of strands with end-to-end distance

\bar{r} for those chains having a contour length $N_j l$, $M_{0j}(\bar{r})$ is the number of strands with end-to-end distance \bar{r} for those chains having a contour length $N_j l$ without external perturbation, i.e., $\gamma_i = 0$. M_1 and M_2 are the total numbers of chains with contour lengths $N_1 l$ and $N_2 l$, respectively. Note that these parameters are determined by the physical and chemical conditions during the preparation of the network. The total number of strands of each contour length is constant; these constraints are taken into account by the Lagrangian multiples $(\mu_j - 1)$. The last term in eq 1 introduces n discrete macroscopic constraints, e.g., mean square or mean end-to-end distances. These constraints depend on the specific stretching experiment and couple the two ensembles with different chain lengths. The corresponding Lagrangian multipliers are γ_i . Λ is the diagonal matrix with the three deformation ratios λ_i ($\Lambda_{ij} = \delta_{ij} \lambda_i$), which determine the macroscopic state of the deformed system under consideration.

As macroscopic constraint we choose $g_i(\bar{r}) = r_i^2$, $i = x, y, z$, in order to have a simple mathematical description (compare refs 7 and 8).

In equilibrium, the entropy assumes an extremum, which is calculated by setting the variational derivatives of the entropy with respect to the distributions $M_j(\bar{r})$ equal to zero. The straightforward calculation yields

$$M_j(\bar{r}) = M_j \exp\{S_{sj}(\bar{r}) + \sum_{n=1}^n \gamma_i g_i(\bar{r})\} \quad (2)$$

For Gaussian chains the entropy is $S_{sj}(\bar{r}) = S_{0j} - a_j \bar{r}^2$ and $a_j = 3/(2N_j l^2)$. Therefore, the Lagrange multipliers γ_i are obtained from

$$\frac{\lambda_i^2}{2} \sum_{j=1}^2 \frac{M_j}{a_j} = \frac{1}{2} \sum_{j=1}^2 \frac{M_j}{a_j - \gamma_i} \quad (3)$$

With the abbreviations $w = M_2/M_1$ and $v = a_2/a_1$ we immediately obtain

$$\beta_i = \frac{\gamma_i}{a_1} = \frac{1+v}{2} - \frac{1+w}{2(1+\frac{w}{v})\lambda_i^2} - \frac{1}{2\sqrt{(v-1)^2 - \frac{2v(v-1)(w-1)}{(w+v)\lambda_i^2} + \frac{v^2(w+1)^2}{(w+v)^2\lambda_i^4}}} \quad (4)$$

and the stress (free energy $F = U - TS = -TS$, $U = 0$, $m = x, y, z$)

$$\sigma_m = \frac{dF}{d\lambda_m} = 2k_B T M_1 \left(1 + \frac{w}{v} \right) \sum_{i=1}^3 \beta_i \lambda_i \frac{d\lambda_i}{d\lambda_m} \quad (5)$$

Figures 1–4 show the fit of this bimodal model to the

* Abteilung Theoretische Physik, Universität Ulm, Albert-Einstein-Allee 11, 89081 Ulm, Germany.

† Abstract published in *Advance ACS Abstracts*, July 1, 1995.

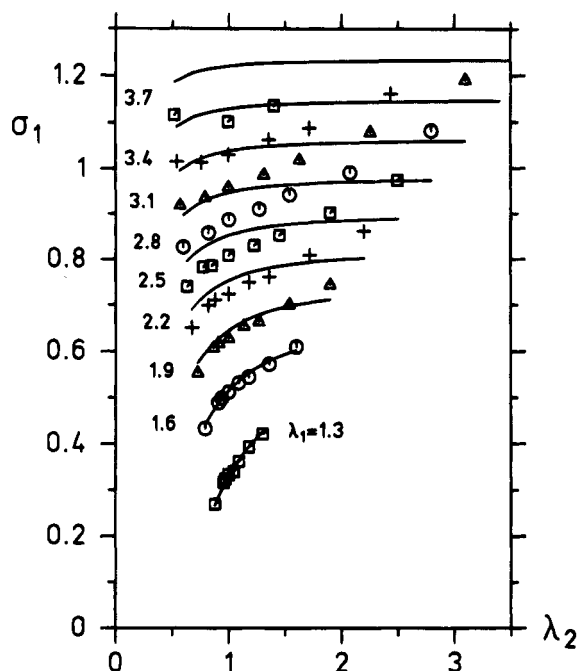


Figure 1. Nonaffine model with two strand lengths: stress σ_1 versus λ_2 (large deformation regime). The experimental points are from Kawabata.¹⁰ The theoretical curves are according to eq 5 with parameters $2k_B TM_1 = 0.210$, $w = 1.48$, and $\nu = 3.12$.

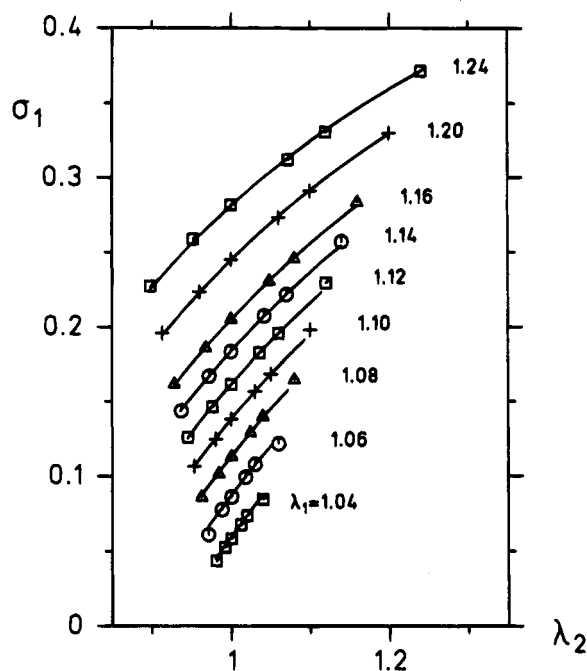


Figure 2. Nonaffine model with two strand lengths: stress σ_1 versus λ_2 (small deformation regime). The experimental points are from Kawabata.¹⁰ The theoretical curves are according to eq 5 with parameters $2k_B TM_1 = 0.210$, $w = 1.48$, and $\nu = 3.12$.

biaxial, i.e., $\lambda_3 = (\lambda_1 \lambda_2)^{-1}$, experimental data of Kawabata.¹⁰ The figures for the small extension regime show very good agreement between theory and experiment! The model obviously fits the *biaxial* data very well. If it were not yet known that samples of vulcanized rubber have a broad distribution of strands of different lengths, this good agreement of the model with the data would strongly suggest such an assumption. The large $w = M_2/M_1$ value means—together with $\nu \approx 3$ —that shorter strands occur more frequently in the material.

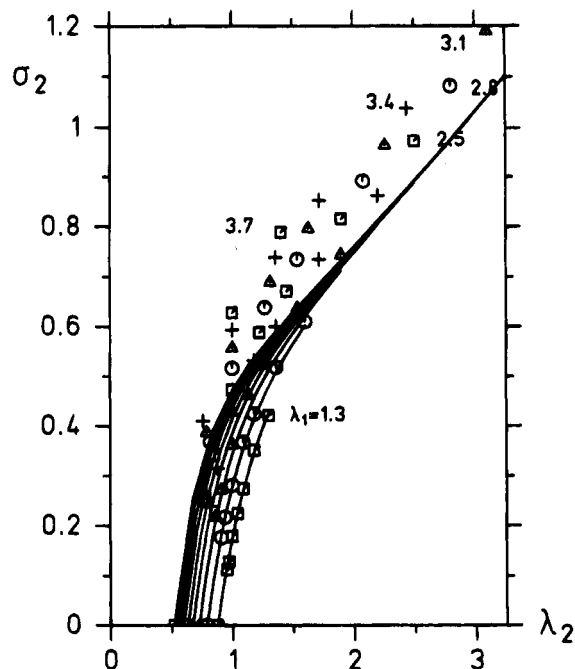


Figure 3. Nonaffine model with two strand lengths: stress σ_2 versus λ_2 (large deformation regime). The experimental points are from Kawabata.¹⁰ The theoretical curves are according to eq 5 with parameters $2k_B TM_1 = 0.210$, $w = 1.48$, and $\nu = 3.12$.

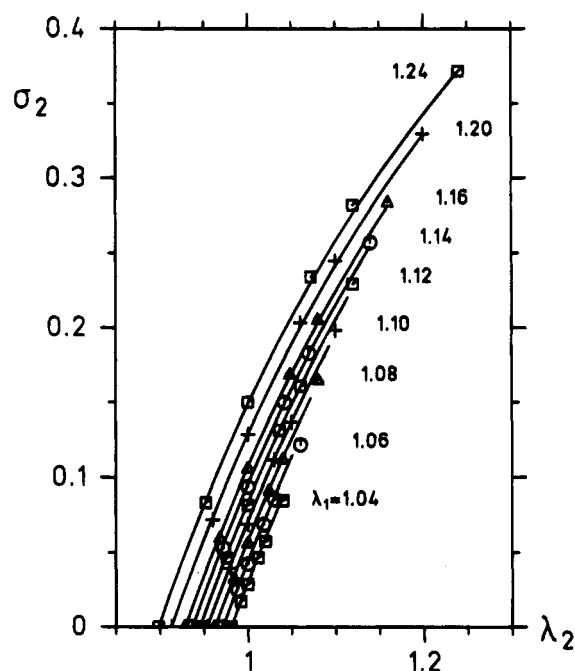


Figure 4. Nonaffine model with two strand lengths: stress σ_2 versus λ_2 (small deformation regime). The experimental points are from Kawabata.¹⁰ The theoretical curves are according to eq 5 with parameters $2k_B TM_1 = 0.210$, $w = 1.48$, and $\nu = 3.12$.

Large extensions, i.e., larger than $\lambda = 1.9$, are not described correctly. This may in part be due to the Gaussian strand model used in the derivation.

Because there are strands of different lengths in the network, it is interesting to investigate the statistical properties of both ensembles. As an example we show in Figure 5 a plot of the mean square end-to-end distances divided by λ^2 for equitriaxial deformation. λ is the deformation ratio ($\lambda = l/l_0$). Parameters are $\nu = 2$ and $w = 1$.

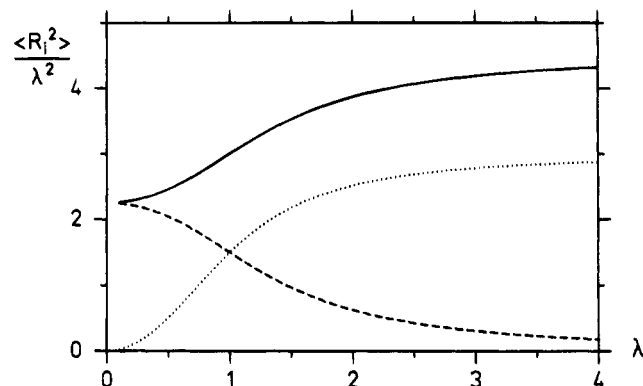


Figure 5. Nonaffine model with two strand lengths, $N_1 = 2N_2$, $M_1 = M_2$ (triaxial deformation): (—) $\langle R_1^2 \rangle / \lambda^2$ (longer strands); (---) $\langle R_2^2 \rangle / \lambda^2$ (shorter strands); (···) $\langle R_2^2 \rangle (!)$ (shorter strands).

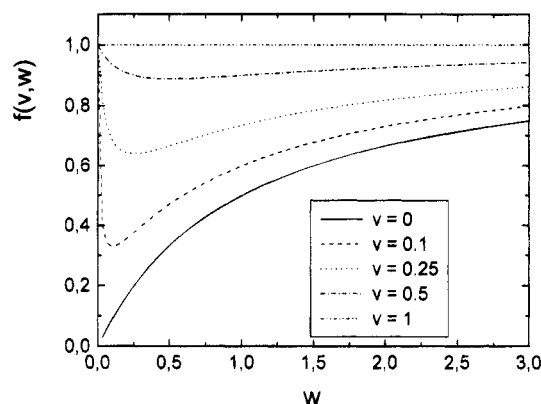


Figure 6. Dependence of modulus on w .

Obviously, the mean square end-to-end distance for the system of the shorter strands reaches a saturation for $\lambda \approx 2$; i.e., for larger extensions their mean square end-to-end distance does not change with deformation. The macroscopic deformation of the total network is produced in this region only by the longer strands. For small deformations $\lambda \approx 1$ the shorter strands contribute to the macroscopic deformation, but their contribution is smaller than in the affine case.

These results for a multichain model are consistent with results obtained by Göritz et al.¹¹ on the basis of a two-chain model.

In the following the dependence of the modulus in uniaxial deformation on the relative chain number w and relative chain length $v = N_1/N_2 (<1)$ is investigated. Comparison to experimental data, e.g., ref 12, is not possible because the modulus depends upon the number of strands $M_1 + M_2$, which is not specified in the publications.

For uniaxial deformation and constant volume, i.e., $\lambda_y = \lambda_z = 1/\lambda_x^{1/2}$ a Taylor expansion of eq 5 at $\lambda_x \approx 1$ yields

$$\sigma_m = 2k_B T (M_1 + M_2) f(v, w) \left(\lambda_x - \frac{1}{\lambda_x^2} \right) \quad (6a)$$

$$f(v, w) = \frac{(w + v)^2}{(1 + w)(w + v^2)} \quad (6b)$$

Figures 6 and 7 show the dependence of $f(v, w)$ on both relative parameters. The modulus as a function of w exhibits a minimum (entropic effect) for fixed v . This is reasonable, because, as is well established, the network modulus does not depend on the modulus of

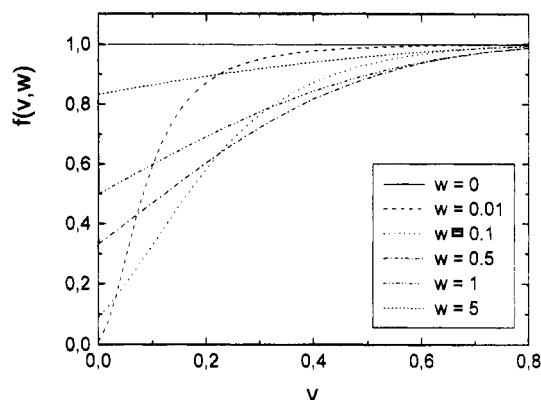


Figure 7. Dependence of modulus on v .

the single chain. Therefore the moduli for $w = 0$ and $w = \infty$ are equal, since only one type of chain exists.

3. Polydisperse Networks

In contrast to the model of the last section we now investigate a network which is not cross-linked from a melt of two different chains, but which polymerized from a soup of monomers. The polymerization is controlled by various chemical parameters. These parameters are projected on just two in the following model: the number of strands M at the end of the polymerization and the number of initial monomers N_g .

In analogy to eq 1 the entropy now reads

$$\begin{aligned} S_{\text{net}}(\Lambda) = & k_B \int M(N, \bar{r}) S_s(N, \bar{r}) d^3r dN + \\ & k_B \{ M \ln M - \int M(N, \bar{r}) \ln M(N, \bar{r}) d^3r dN \} + \\ & k_B (\mu - 1) \{ M - \int M(N, \bar{r}) d^3r dN \} + \\ & k_B \bar{\mu} \{ N_g - \int M(N, \bar{r}) N d^3r dN \} + \\ & k_B \sum_{i=1}^n \gamma_i \{ \int M(N, \bar{r}) g_i(\bar{r}) d^3r dN - \\ & \int M_0(N, \bar{r}) g_i(\Lambda \bar{r}) d^3r dN \} \quad (7) \end{aligned}$$

$M(N, \bar{r})$ is the distribution function of strands consisting of N monomers and having end-to-end distance \bar{r} . $M_0(N, \bar{r})$ is the equilibrium distribution without external constraints, i.e. $\gamma_i = 0 \forall i$. In addition to eq 1 the fixed monomer number N_g is accounted for by the Lagrangian multiplier $\bar{\mu}$.

3.1. Calculation of the Distribution $M_0(N, \bar{r})$ without External Constraints. The variations of eq 7 with respect to the distribution $M(N, \bar{r})$ leads to (with $\gamma_i = 0 \forall i$)

$$M_0(N, \bar{r}) = M \frac{e^{-\bar{\mu}N + S_s(N, \bar{r})}}{\int e^{-\bar{\mu}N + S_s(N, \bar{r})} d^3r dN} \quad (8)$$

where we already eliminated μ . Within the Gaussian approximation

$$S_s(N, \bar{r}) = S_0 - \frac{3}{2Nl^2} \bar{r}^2 - \frac{3}{2} \ln N \quad (9)$$

we find from eq 8 $\bar{\mu} = M/N_g$ and

$$M_0(N) = \int M_0(N, \bar{r}) d^3r = \frac{M^2}{N_g} e^{-(M/N_g)N} \quad (10)$$

$M_0(N)$ is the number of strands of contour length N being generated during a polymerization starting with

N_g monomers and ending with M strands and resulting finally at an extremum of the entropy. The fact that the distribution of chain lengths in such systems decays exponentially is numerically verified.^{13,14} This shows that the model introduced above describes polymerization quite well.

3.2. Deformation after Cross-Linking. After cross-linking, we are no longer allowed to use eq 7, because then the number of strands of length N is fixed. Equation 7 describes the case where the strand distribution $M(N, \bar{r})$ can change during deformation. This is the case for physical cross-links. Here we assume that we have only chemical cross-links and therefore $M_0(N)$ is fixed. Thus the constraints due to the Lagrange multipliers μ and $\bar{\mu}$ must be substituted by the following term

$$\int dN \bar{\gamma}(N) \{M_0(N) - \int M(N, \bar{r}) d^3r\} \quad (11)$$

with an infinite number of Lagrange multipliers $\bar{\gamma}(N)$.

3.3. Quasiaffine Case. In the quasiaffine case the macroscopic constraints are fulfilled for every function $g_i(\bar{r})$.^{7,9} Obvious mathematical transformations of the corresponding constraints lead to

$$M(N, \bar{r}) = \frac{1}{\sqrt{I_3}} M_0(N, \Lambda^{-1} \bar{r}) \quad (12)$$

resulting in the following stress-strain relation

$$\sigma_m = \frac{Mk_B T}{2} \frac{d}{d\lambda_m} \{I_1 - \ln I_3\} \quad (13)$$

with $I_1 = \lambda_x^2 + \lambda_y^2 + \lambda_z^2$ and $I_3 = \lambda_x^2 \lambda_y^2 \lambda_z^2$. Equation 13 is identical to the well-known result first obtained by Wall¹⁵ for a unimodal network.⁹ Therefore one cannot distinguish between unimodal and multimodal networks in considering the stress-strain relation of the quasiaffine case. This is probably due to the infinite number of constraints.

3.4. Special Case: $g_i(\bar{r}) = |\mathbf{r}_i|$. Variation of the entropy with $g_i(\bar{r}) = |\mathbf{r}_i|$ yields ($a = 3/2(Nl^2)$)

$$M(N, \bar{r}) = \frac{M^2}{8N_g} e^{-(N/N_g)M} \left\{ \frac{3}{2\pi Nl^2} \right\}^{3/2} \prod_{i=x,y,z} \frac{e^{-\gamma_i^2/4a}}{1 + \operatorname{erf}\left(\frac{\gamma_i}{2\sqrt{a}}\right)} e^{-a\mathbf{r}_i^2 + \gamma_i |\mathbf{r}_i|} \quad (14)$$

resulting in a transcendental equation for the calculation of γ_i . A Padé approximation in the equation determining γ_i (correct limiting cases for $\lambda \rightarrow \infty$ and $\lambda \rightarrow 0$ and agreement for $\lambda = 1$ to the exact transcendental equation) results in

$$\sigma_m = \frac{Mk_B T}{2} \frac{d}{d\lambda_m} \left\{ \frac{I_1}{2} + (\lambda_x + \lambda_y + \lambda_z) - \ln I_3 \right\} \quad (15)$$

The important fact of eq 15 is its universality in the sense that it depends only on the number M of network strands. A comparison of this result with the experimental data of Kawabata¹⁰ is not shown, because for deformations up to $\lambda_1 \approx 1.6$ the agreement is as well as

in Figures 1–4. For large extensions one cannot expect agreement because of the Gaussian approximation used for the strands.

4. Summary

In this paper we gave examples of how to incorporate polydispersity in the network model introduced recently,^{7–9} which describes the polymer network as a gas of chains subject to macroscopic constraints.

We investigated a bimodal as well as a multimodal network using the maximum entropy principle for given monomer and strand numbers. Both models result in an excellent fit to biaxial stress-strain experiments of vulcanized rubber in the Gaussian regime and show the Mooney effect. This excellent agreement is achieved in the bimodal network through a fit of the relative contour lengths and the relative numbers of both types of strands. For a multimodal network the same good agreement with experimental data is obtained although there is just one parameter in the model, which is the number of strands. Therefore one might conclude that the Mooney effect is a consequence of polydispersity. However, this point should not be overestimated, because inclusion of the network functionality,^{7,16} yields a similar effect also for the “monodisperse” model network.

The main advantage of the model is its conceptual simplicity, i.e., entropy maximization under constraints. This straightforward method allows also the calculation of the functionality dependence, swelling experiments,^{7,8,16} and with the help of the strands distribution $M(N, \bar{r})$, neutron scattering experiments. A shortcoming might be that the macroscopic behavior is not explicitly related to microscopic mechanisms.

Acknowledgment. This work was supported by the Deutsche Forschungsgemeinschaft (DFG) within Sonderforschungsbereich (SFB) 239. Helpful discussions with Prof. Dr. H.-G. Kilian are gratefully acknowledged.

References and Notes

- (1) Treloar, L. R. G. *The Physics of Rubber Elasticity*; Clarendon Press: Oxford, U.K., 1975.
- (2) Kilian, H.-G. *Polymer* **1981**, *22*, 209.
- (3) Ball, R. C.; Doi, M.; Edwards, S. F.; Warner, M. *Polymer* **1981**, *22*, 1010.
- (4) Graessley, W. W. *Adv. Polym. Sci.* **1982**, *47*, 67.
- (5) Gottlieb, M.; Gaylord, R. J. *Polymer* **1983**, *24*, 1644.
- (6) Edwards, S. F.; Vilgis, Th. *Polymer* **1986**, *26*, 101.
- (7) Glatting, G. Ph.D. Dissertation, Universität Ulm, Germany, 1992.
- (8) Glatting, G.; Winkler, R. G.; Reineker, P. *Macromol. Symp.* **1994**, *81*, 129.
- (9) Glatting, G.; Winkler, R. G.; Reineker, P. *J. Chem. Phys.* **1994**, *101*, 2532.
- (10) Kawabata, S.; Matsuda, M.; Tei, K.; Kawai, H. *Macromolecules* **1981**, *14*, 154.
- (11) Göritz, D.; Sommer, J.-U.; Duschl, E. J. *KGK Kautsch. Gummi Kunstst.* **1994**, *47*, 170.
- (12) Mark, J. E. *Adv. Polym. Sci.* **1982**, *44*, 1.
- (13) Schulz, M. Ph.D. Dissertation, TH Merseburg, Germany, 1988.
- (14) Schulz, M.; Sommer, J.-U. *J. Chem. Phys.* **1992**, *96*, 7102.
- (15) Wall, F. T. *J. Chem. Phys.* **1943**, *11*, 527.
- (16) Glatting, G.; Winkler, R. G.; Reineker, P. *Submitted for publication*.

MA9463371